JOC*Article*

Mode Selectivity in the Intramolecular Cyclization of Ketenimines Bearing *N*-Acylimino Units: A Computational and Experimental Study

Mateo Alajarín,* Pilar Sánchez-Andrada,* Angel Vidal, and Fulgencio Tovar

Departamento de Química Orgánica, Facultad de Química, Campus de Espinardo, Universidad de Murcia, 30100 Murcia, Spain

alajarin@um.es

Received October 1, 2004

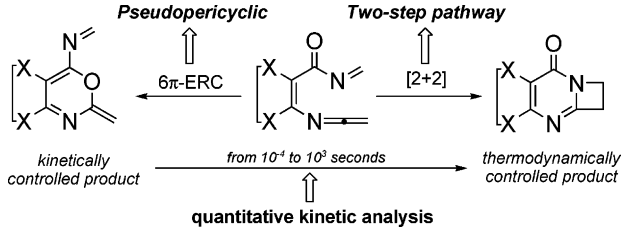

The mode selectivity in the intramolecular cyclization of a particular class of ketenimines bearing *N*-acylimino units has been studied by ab initio and DFT calculations. In the model compounds the carbonyl carbon atom and the keteniminic nitrogen atom are linked either by a vinylic or an *o*-phenylene tether. Two cyclization modes have been analyzed: the [2+2] cycloaddition furnishing compounds with an azeto[2,1-*b*]pyrimidinone moiety and a 6π-electrocyclic ring closure leading to compounds enclosing a 1,3-oxazine ring. The [2+2] cycloaddition reaction takes place via a two-step process with formation of a zwitterionic intermediate, which has been characterized as a cross-conjugated mesomeric betaine. The 6π-electrocyclic ring closure occurs via a transition state whose pseudopericyclic character has been established on the basis of its magnetic properties, geometry, and NBO analysis. The 6π-electrocyclic ring closure is energetically favored over the [2+2] cycloaddition, although the [2+2] cycloadducts are the thermodynamically controlled products. A quantitative kinetic analysis predicts that 1,3-oxazines would be the kinetically controlled products, but they should transform rapidly and totally into the [2+2] cycloadducts at room temperature. In the experimental study, a number of *N*-acylimino-ketenimines, in which both reactive functions are supported on an *o*-phenylene scaffold, have been successfully synthesized in three steps starting from 2-azidobenzoyl chloride. These compounds rapidly convert into azeto[2,1-*b*]quinazolin-8-ones in moderate to good yields as a result of a formal [2+2] cycloaddition.

Introduction

N-Acylimines and *N*-acyliminium ions[1] behave as valuable imino dienophiles when confronted with all-carbon dienes in [4+2] cycloaddition reactions leading to tetrahydropyridines.[2] They may also act as the 4π component in hetero-Diels–Alder reactions of inverse electronic demand involving the combination of these species as electron-deficient heterodienes (in neutral or, more commonly, protonated form) with electron-rich dienophiles.[3] However, the participation of the C=N bond of *N*-acylimines in [2+2] cycloaddition reactions is rare. To our knowledge, the only reported reaction of this type is the catalyzed [2+2] cycloaddition of *N*-acylimines with ketenes yielding β-lactams, recently disclosed by Lectka and co-workers.[4]

Our interest in the study of the intramolecular [2+2] cycloaddition reactions between imines and ketenimines,[5]

(1) For a recent review about the cyclizations of *N*-acyliminium ions see: Maryanoff, B. E.; Zhang, H.-C.; Cohen, J. H.; Turchi, I. J.; Maryanoff C. A. *Chem. Rev*. **2004**, *104*, 1431–1628.

(2) (a) Boger, D. L.; Weinreb, S. M. *Hetero Diels–Alder Methodology in Organic Synthesis*; Academic Press: San Diego, CA, 1987; Chapter 2. (b) *Organic Synthesis Highlights II*; Waldmann, H., Ed.; VCH Verlagsgesellschaft: Weinheim, Germany, 1995; pp 37–47. (c) Kametani, T.; Hibino, S. *Adv. Heterocycl. Chem.* **1987**, *42*, 245–333. (d) Whiting, A.; Windsor, C. M. *Tetrahedron* **1998**, *54*, 6035–6050. (e) Khatri, N. A.; Schmitthenner, H. F.; Shringarpure, J.; Weinreb, S. *J. Am. Chem. Soc*. **1981**, *103*, 6387–6393.

(3) (a) Weinreb, S. M.; Scola, P. M. *Chem. Rev.* **1989**, *89*, 1525–1534. (b) Gizecki, P.; Dhal, R.; Poulard, C.; Gosselin, P.; Dujardin, G. *J. Org. Chem.* **2003**, *68*, 4338–4344. (c) Gong, Y.; Bausch, M. J.; Wang, L. *Tetrahedron Lett.* **2001**, *42*, 1–4. (d) Michels, G.; Hermesdorf, M.; Schneider, J.; Regitz, M. *Chem. Ber*. **1988**, *121*, 1775–1783.

(4) (a) Dudding, T.; Hafez, A. M.; Taggi, A. E.; Wagerle, T. R.; Lectka, T. *Org. Lett*. **2002**, *4*, 387–390. (b) Hafez, A. M.; Taggi, A. E.; Dudding, T.; Lectka, T. *J. Am. Chem. Soc.* **2001**, *123*, 10853–10859.

10.1021/jo0482716 CCC: $30.25
Published on Web 01/15/2005

SCHEME 1. Planned Intramolecular [2+2] Cycloaddition of *N*-Acylimino-ketenimines

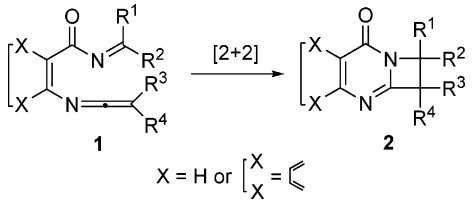

and the particular electronic characteristics of *N*-acylimines (see below), led us to explore, theoretically and experimentally, if the C=N bond of an *N*-acylimine would participate in a [2+2] intramolecular cycloaddition with a ketenimine function. To this end, we planned placing both functionalities on a *Z*-1,2-vinylic or *o*-phenylene scaffold as represented in structure **1** (Scheme 1), as our previous work in the intramolecular cyclization of other imino-ketenimines supported in similar frameworks occurred successfully.[5] If successful, these cycloadditions should lead to adducts **2**.

It has been demonstrated that the *intermolecular* [2+2] cycloadditions of ketenimines with imines yielding azetidin-2-imines only takes place if the ketenimines bear electron-withdrawing substituents at the nitrogen atom, which increase their electrophilic character.[6] By contrast, we demonstrated that the intramolecular [2+2] cycloaddition of imino-ketenimines is considerably easier than the intermolecular version if both functional groups are incorporated into an appropriate scaffold, and does not require the presence of electron-withdrawing groups on the ketenimine nitrogen.[5]

A common nonconcerted mechanism has been established[5c−e,7] for all the [2+2] cycloaddition reactions of imino-ketenimines that have been approached by computational methods. For example, the conversion of *N*-(4-azapenta-1,4-dienyl)ketenimine (**3**) into its [2+2] cycloadduct **4** takes place in two steps. The first one involves the nucleophilic attack of the iminic nitrogen lone pair onto the central carbon atom of the ketenimine moiety, leading to a zwitterionic intermediate **INT** that, in the second step, undergoes a 4π-conrotatory ring closure (Scheme 2). The conjugated C=C bond linked to the keteniminic nitrogen enhances the electrophilic character of the ketenimine moiety favoring the cyclization process.[5c]

We have found in the literature several reports dealing with the electronic description and the rotational profile of the simplest *N*-acylimine, methyleneformamide.[8] Interestingly, its computed global minimum energy conformation is *s*-cisoid, and it shows a torsional angle θ_{CNCO}

SCHEME 2. [2+2] Cycloaddition of the Imino-ketenimine 3 Leading to Bicycle 4

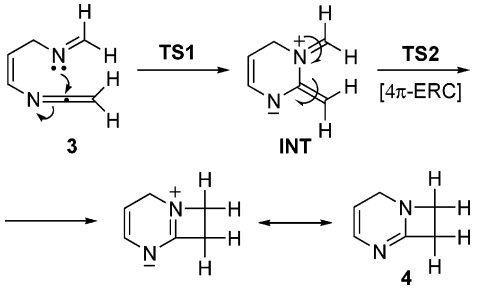

close to 50°. By contrast, the *s*-trans conformer is the global minimum energy conformation of 2-azabutadiene. Wiberg[8a] stated that the delocalization index of the lone pair at the nitrogen atom in methyleneformamide is higher than that of the 2-azabutadiene. This fact was explained by the greater electron-withdrawing character of the C=O bond when compared with the C=C bond, accounting for the calculated minimum energy conformation that allows the partial delocalization of the nitrogen lone pair into the C=O bond as well as some conjugation between the C=N and the C=O π-systems. Other reports on the structure and conformation of more complex *N*-acylimines support these hypotheses.[9]

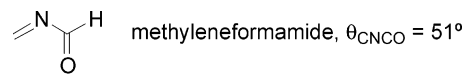

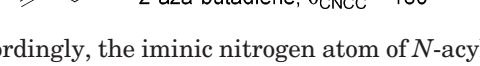

Accordingly, the iminic nitrogen atom of *N*-acylimines is probably less nucleophilic than that of simple imines where it is linked to an sp^3-hybridized carbon atom and, hence, the [2+2] cycloaddition reactions of *N*-acylimino-ketenimines type **1** seem a priori more difficult than those of the previously essayed imino-ketenimines represented by structure **3**. Nevertheless, the tether linking the *N*-acylimine and the ketenimine moieties in the imino-ketenimines **1**, an *o*-phenylene or vinylic fragment, may increase the electrophilic character of the ketenimine moiety by communicating across its π-system the C=O function with the N=C π-system of the ketenimine component. This feature might compensate the presumably poor nucleophilic character of their iminic nitrogen atom.

On the other hand, an alternative cyclization mode of *N*-acylimino-ketenimines **1** that can be envisaged is the 6π-electrocyclic ring closure leading to the [1,3]-oxazine **5** (Scheme 3). Moreover, due to its likely pseudopericyclic character,[10] a low-energy barrier can be presumed for this transformation.

(5) (a) Alajarín, M.; Molina, P.; Vidal, A. *Tetrahedron Lett.* **1996**, *37*, 8945−8948. (b) Alajarín, M.; Molina, P.; Vidal, A.; Tovar, F. *Tetrahedron* **1997**, *53*, 13449−13472. (c) Alajarín, M.; Vidal, A.; Tovar, F.; Arrieta, A.; Lecea, B.; Cossío, F. P. *Chem. Eur. J.* **1999**, *5*, 1106−1117. (d) Cossío, F. P.; Arrieta, A.; Lecea, B.; Alajarín, M.; Vidal, A.; Tovar, F. *J. Org. Chem.* **2000**, *65*, 3633−3643. (e) Alajarín, M.; Vidal, A.; Tovar, F.; Cossío, F. P.; Arrieta, A.; Lecea, B. *J. Org. Chem.* **2000**, *65*, 7512−7515. (f) Alajarín, M.; Vidal, A.; Orenes, R.-A. *Eur. J. Org. Chem.* **2002**, 4222−4227.

(6) (a) Arnold, B.; Regitz, M. *Angew. Chem., Int. Ed. Engl.* **1979**, *18*, 320. (b) Van Camp, A.; Goossens, D.; Moya-Portugez, M.; March-and-Brynaert, J.; Ghosez, L. *Tetrahedron Lett.* **1980**, *21*, 3081−3084.

(7) (a) Alajarín, M.; Sánchez-Andrada, P.; Vidal, A.; Tovar, F. *Eur. J. Org. Chem.* **2004**, 2636−2643. (b) Alajarin, M.; Vidal, A.; Tovar, F.; Sánchez-Andrada, P. *Tetrahedron Lett.* **2002**, *43*, 6259−6261.

(8) (a) Wiberg, K. B.; Rablen, P. R.; Marquez, M. *J. Am. Chem. Soc.* **1992**, *114*, 8654−8668. (b) See also: Allmann, R.; Kupfer, R.; Nagel, M.; Würthwein, E.-U. *Chem. Ber.* **1984**, *117*, 1597−1605. (c) Würthwein, E.-U.; Kupfer, R.; Kaliba, C. *Angew. Chem., Int. Ed. Engl.* **1983**, *22*, 252−253. (d) McAllister, M. A.; Tidwell, T. *J. Chem. Soc., Perkin Trans. 2* **1994**, 2239−2248.

(9) See for example: (a) Gross, L. A.; Baird, G. S.; Hoffman, R. C.; Baldridge, K. K.; Tsien, R. Y. *Proc. Natl. Acad. Sci.* **2000**, *97*, 11990−11995. (b) Yarbrough, D.; Wachter, R. M.; Kallio, K.; Matz, M. V.; Remington, S. J. *Proc. Natl. Acad. Sci.* **2001**, *98*, 462−467.

(10) (a) Birney, D. M. *J. Org. Chem.* **1996**, *61*, 243−251. (b) Alajarín, M.; Sánchez-Andrada, P.; Cossío, F. P.; Arrieta, A.; Lecea, B. *J. Org. Chem.* **2001**, *66*, 8470−8477.

TABLE 1. Energy Barriers (ΔE, kcal·mol^{-1}) Computed for the Reactions Included in Schemes 2, 4, and 5[a]

1a → **2a** and **1a** → **5a**	ΔE_{1a}	ΔE_{INTa}	ΔE_{2a}	ΔE_{rxn2a}	ΔE_{3a}	ΔE_{rxn5a}
HF/6-31G* [b]	20.10	0.99	23.80	−45.38	15.89	−12.19
MP2/6-31G* [c]	10.25	−10.40	12.18	−51.06	8.33	−14.25
B3LYP/6-31G* [d]	7.43	−9.49	15.14	−43.82	4.88	−14.36
1b → **2b** and **1b** → **5b**	ΔE_{1b}	ΔE_{INTb}	ΔE_{2b}	ΔE_{rxn2b}	ΔE_{3b}	ΔE_{rxn5b}
HF/6-31G* [b]	23.51	12.91	17.26	−46.41	21.71	5.70
MP2/6-31G* [b]	14.64	4.66	4.08	−50.62	15.61	7.11
B3LYP/6-31G* [d]	11.38	0.08	9.06	−44.78	9.94	−0.10
3 → **4**[5c]	ΔE_1	ΔE_{INT}	ΔE_2	ΔE_{rxn4}		
HF/6-31G* [b]	32.18	24.49	20.00	−24.38		
MP2/6-31G* [b]	18.25	12.83	7.44	−30.34		
B3LYP/6-31G* [d]	19.73	14.04	11.06	−22.57		

[a] See Figure 1 for the notation of the energy barriers. [b] Energies computed on the fully optimized HF/6-31G* geometries. The ZPVE corrections, computed at the same level, have been included. The ZPEs were not scaled. [c] Energies computed on the fully optimized MP2/6-31G* geometries. The ZPVE corrections, computed at the same level, have been included. The ZPEs were not scaled. [d] Energies computed on the fully optimized B3LYP/6-31G* geometries. The ZPVE corrections, computed at the same level, have been included. The ZPEs were not scaled.

SCHEME 3. The Two Cyclization Modes of *N*-Acylimino-ketenimines 1

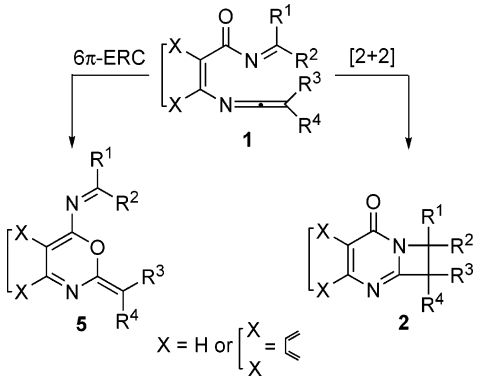

Here, we report the computational and the experimental study undertaken with the aim of exploring the mode selectivity ([2+2] cycloaddition vs 6π-electrocyclic ring closure) in the intramolecular cyclization of *N*-acylimino-ketenimines **1** and its mechanistic scheme.

Computational Results

For the theoretical study we selected the most simple systems that model the *N*-acylimino-ketenimines **1**, those where the iminic carbon atom and the terminal atom of the ketenimine moiety are unsubstituted and the two reactive functionalities are linked either by a vinylic (**1a**) or an *o*-phenylene (**1b**) tether (Scheme 4). We carried out an intensive search along the RHF/6-31G*, B3LYP/6-31G*, and MP2/6-31G* potential energy surfaces for the transformations of **1a** into **2a** and **5a**, whereas for the transformations of **1b** into **2b** and **5b** the search was made along the RHF/6-31G* and the B3LYP/6-31G* potential energy surfaces, and the MP2/6-31G* calculations were computed on the fully optimized RHF/6-31G* geometries. The energy barriers computed at the B3LYP and MP2 theoretical levels were similar, in general somewhat higher at the MP2 level, and are gathered in Table 1. The qualitative reaction profiles are depicted in Figure 1. In Figures 2 and 3 the chief geometrical features of the corresponding stationary points optimized at the B3LYP level are shown. With the aim of simplifying the discussion we will comment on only the results obtained at the B3LYP/6-31G* theoretical level, unless otherwise stated. Houk et al. have shown that this computational level is adequate for pericyclic reactions, its quality being comparable or even superior to that of comparatively more expensive methods.[11]

SCHEME 4. The Two-Step Pathway Found for the [2+2] Cycloaddition of the *N*-Acylimino-ketenimines 1a,b Leading to the Cycloadducts 2a,b

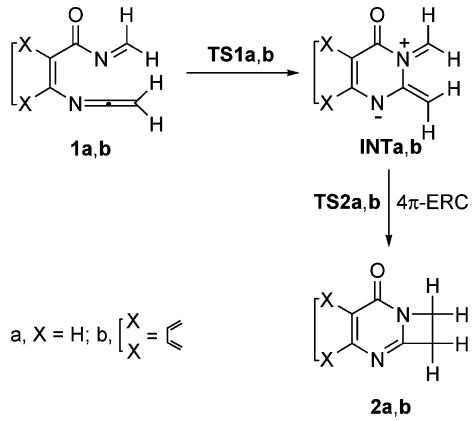

The Two-Step [2+2] Cycloaddition Pathway. For the transformations of **1a**,**b** into the [2+2] cycloadducts **2a**,**b** this computational study provides reaction pathways similar to those previously described for the intramolecular [2+2] cycloaddition of other imino-ketenimines,[5c] involving the zwitterionic intermediates **INTa**,**b** shown in Scheme 4 and the corresponding transition structures **TS1a**,**b** and **TS2a**,**b**.

For the sake of comparison, in Table 1 we also gathered the energy barriers computed previosly[5c] for the conversion of *N*-(4-azapenta-1,4-dienyl)ketenimine (**3**) into its [2+2] cycloadduct **4** (Scheme 2), where a methylene sp^3-carbon is linked to the iminic N atom instead of the carbonyl sp^2-carbon in **1a**,**b**.

The computed energy barriers associated to the first step of the [2+2] cycloaddition of *N*-acylimino-keten-

(11) Guner, V.; Khuong, K. S.; Leach, A. G.; Lee, P. S.; Bartberger, M. D.; Houk, K. N. *J. Phys. Chem. A* **2003**, *107*, 11445−11459.

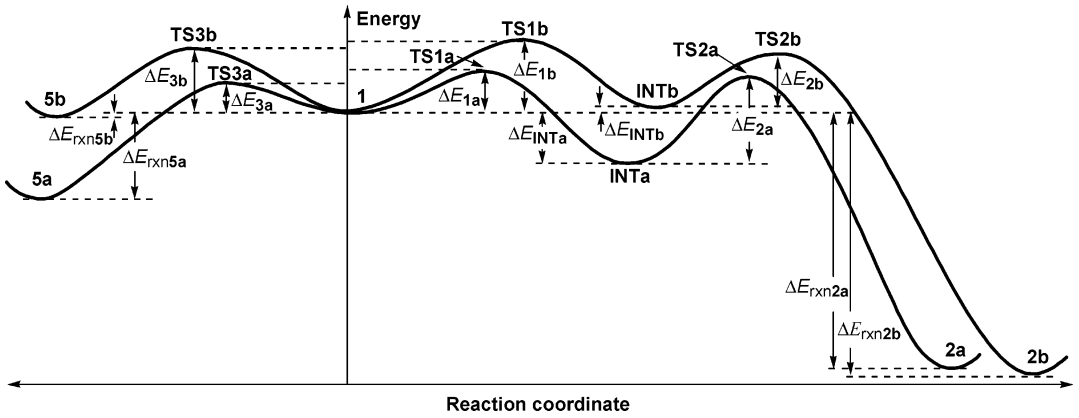

FIGURE 1. Qualitative reaction profiles at the B3LYP/6-31G* level of the intramolecular [2+2] cycloaddition and the 6π-electrocyclic ring closure of *N*-acylimino-ketenimines **1a**,**b** leading to **2a**,**b** and **5a**,**b**, respectively.

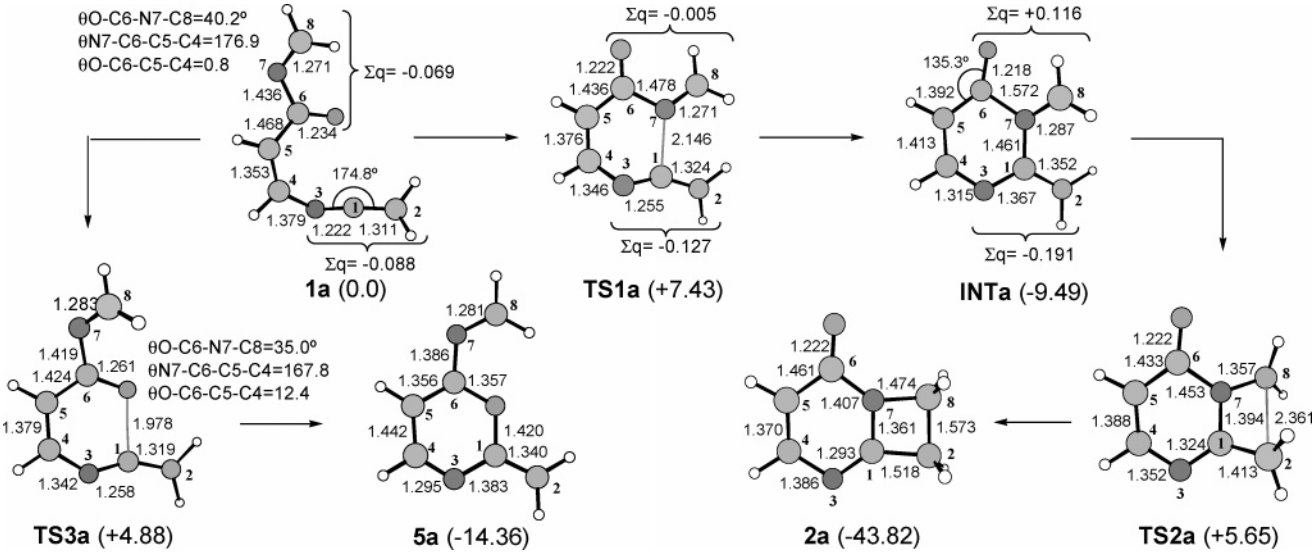

FIGURE 2. Computer plot of the stationary points found in the transformation of *N*-acylimino-ketenimine **1a** into **2a** and **5a** optimized at the B3LYP/6-31G* level. Plain numbers correspond to the geometrical parameters, and the numbers between parentheses are the relative energies. Bond lengths and angles are given in angstroms and degrees, respectively. In this and the following figure that include ball-and-stick representations, atoms are represented by increasing depth of shading in the order H, C, O, and N.

imines **1a**,**b** through the transition structures **TS1a**,**b** were 7.43 and 11.38 kcal·mol^{-1} respectively, both being lower than the barrier computed for the transformation of imino-ketenimine **3** into the polar intermediate **INT** (19.73 kcal·mol^{-1}). The following reasonings on electronics grounds may be argued to account for the relative weights of these energy barriers:

In *N*-acylimino-ketenimines **1a**,**b** the conformation of the *N*-acylimino units is *s*-cisoid, showing a torsional angle θ_{CNCO} close to 40°, a similar value to that of methyleneformamide (see Figures 2 and 3). The conjugation of the C1=N3 π-system occurs not only with the adjacent C4=C5 π-system, but also with the C=O function, resulting in a notable increase of the electrophilic character of the ketenimine moiety: the natural charge on the central carbon of the ketenimine function is lower in the imino-ketenimine **3** (0.40) than in **1a**,**b** (0.45 in both compounds). Interestingly, the nucleophilicity of the iminic nitrogen atom seems to be higher in the *N*-acylimino-ketenimines **1a**,**b** than in **3**: the natural charge on the iminic atom is more negative in **1a**,**b** (−0.49 and −0.50, respectively) than in the imino-ketenimine **3** (−0.42). In consequence a better nucleophile−electrophile interaction between the two reacting fragments is expected for **1a**,**b** when compared with **3**. On the other hand, the conjugation of the C1=N3 π-system with the C=O group in **1b** involves some loss of aromaticity of the benzene ring, and consequently the conjugation between these π-systems is probably lower than that in **1a**. This idea could account for the slightly lower electrophilicity of the ketenimine moiety of **1b** when compared with that of **1a** (see Figures 2 and 3 and Tables S2−S5 of the Supporting Information).

As a consequence of the attack of the iminic nitrogen on the ketenimine central carbon, partial or total positive and negative charges are generated on the iminic and the heterocumulenic parts, respectively, of the first transition states and, obviously, of the polar intermediates. The C=O group present in **TS1a**,**b** and **INTa**,**b** allows for a more efficient charge delocalization than their CH_2-analogous **TS1** and **INT**, as represented by the resonance hybrids in Chart 1. In turn, the delocalization

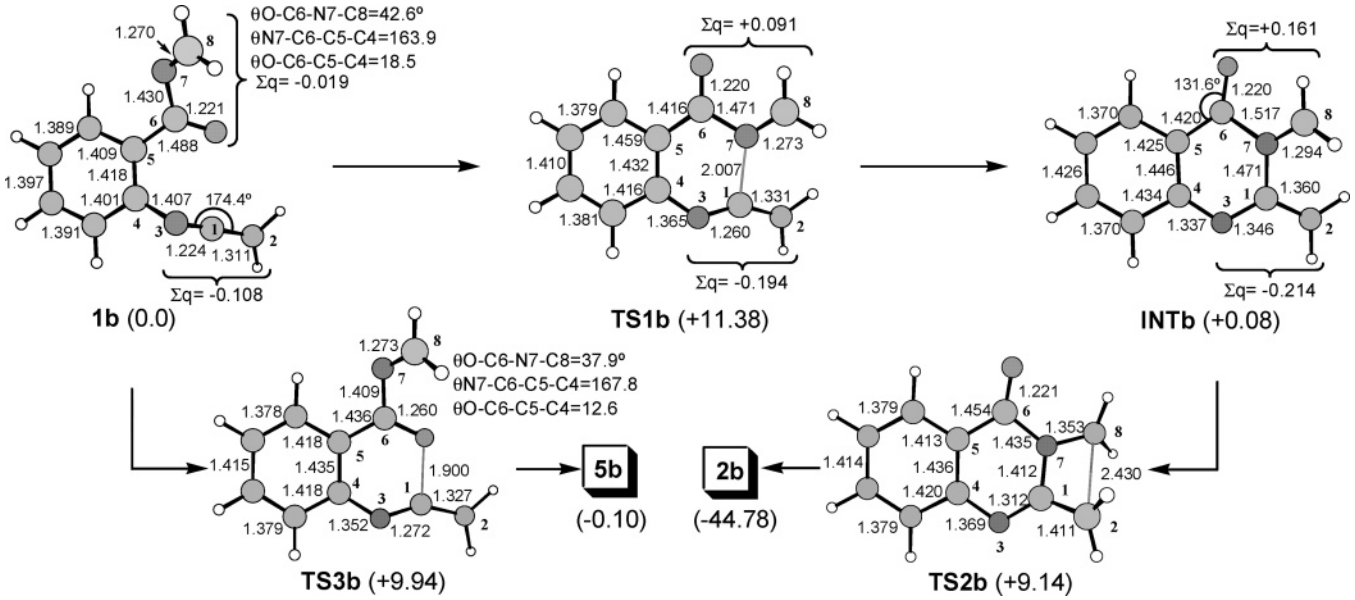

FIGURE 3. Computer plot of the stationary points found in the transformation of *N*-acylimino-ketenimine **1b** into **2b** and **5b**. See the caption of Figure 2 for additional details.

CHART 1. Some Canonical Forms of the Resonance Hybrids 1a,b and INTa,b

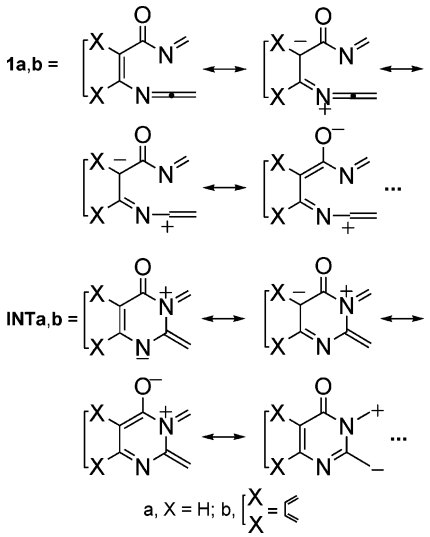

CHART 2. Charge Distribution According to the VB Method of the Cross-Conjugated Mesomeric Betaines INTa,b Showing the Anionic and Cationic Segments and the Two Open-Valence Tautomers 1a,b and 6a,b

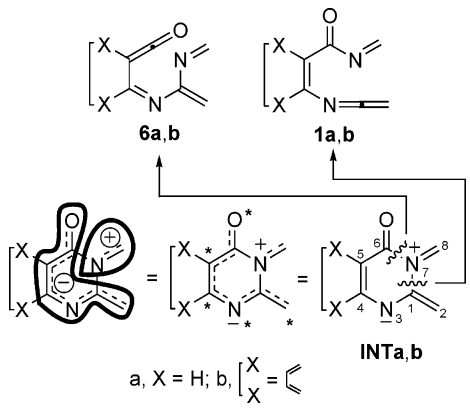

is more effective in **TS1a** and **INTa** than in **TS1b** and **INTb** (see Σ*q* in Figures 2 and 3), probably as a result of the slight loss of aromaticity in the benzene ring necessary for allowing the delocalization of negative charge on the carbonyl oxygen via *o*-quinoid canonical forms. This fact may account for the higher energy barrier computed for the conversion **1b** → **INTb** with respect to that of **1a** → **INTa**.

Before describing the second step of the [2+2] cycloaddition of the *N*-acylimino-ketenimines **1a**,**b**, we will focus now into the special characteristics of the zwitterionic intermediates **INTa**,**b**, which are real heterocyclic mesomeric betaines. Depending on their electronic nature, Ollis classified these compounds into four major classes: conjugated, cross-conjugated, pseudo-cross-conjugated, and heterocyclic *N*-ylides.[12] The subdivision on the basis of the isoconjugated equivalents (see below) led to four additional subclasses for a total of 16 distinct structural types of heterocyclic mesomeric betaines. A detailed analysis of the polar intermediates **INTa**,**b**, and their resonance forms, reveals that the opposite charges are delocalized in separated parts of a common π-electron system, the carbonyl carbon atom acting as an isolator that prevents the charge neutralization. The anionic segment is isoconjugated with an odd alternant hydrocarbon anion (odd-AH, 9 atoms in **INTa** and 13 in **INTb**), therefore these betaines belong to a subclass of cross-conjugated mesomeric betaines (CCMB-odd-AH). In Chart 2 the starred positions indicate the possible sites for the negative charge in the canonical formulas. The positive segment is joined to the negative one by two *union bonds* (C1−N7 and C6−N7) through two unstarred sites. There are two open-chain valence tautomers of these intermedi-

(12) (a) Ollis, W. D.; Stanforth, S. P.; Ramsden, C. A. *Tetrahedron* **1985**, *41*, 2239−2329. See also: (b) Schmidt, A.; Habeck, T.; Kinderman, M. K.; Nieger, M. *J. Org. Chem*. **2003**, *68*, 5977−5982. (c) Potts, K. T.; Murphy, P. M.; Kuehnling, W. R. *J. Org. Chem*. **1988**, *53*, 2889−2898.

ates: the *N*-acylimino-ketenimines **1a**,**b** and the *N*-(2-azabutadien-3-yl)imino-ketenes **6a**,**b** (Chart 2).

Somewhat unexpectedly, we noted a slight similarity between the calculated structure of **INTa** and that presumed for their open-chain valence tautomer **6a**. This finding is inferred from the following observations: (i) a notable increase of the C6−N7 bond distance on going from the imino-ketenimine **1a** to **INTa** (from 1.436 Å to 1.572 Å); (ii) the computed bond order of this bond is low in **INTa** (0.74); and (iii) the C5−C6−O bond angle of **INTa** is wide (135.30°), while the N7−C6−O bond angle is small (114.9°) (see also the bond lengths and the computed bond orders of the bonds forming the six-membered ring in Tables S4 and S5 of the Supporting Information).[13] In contrast, **INTb** is less similar to the structure expected for its valence tautomer, the *o*-quinomethane imine **6b**, than in the preceding case, probably as a result of the partial loss of aromaticity of the benzene ring that such similarity would require.

In relation to the second step of the [2+2] cycloaddition, the computed energy barrier associated to the conrotatory ring closure of **INTa** leading to **2a** via the transition structure **TS2a** was 15.14 kcal·mol^{-1}, a value higher than those computed for the conversion of the intermediates **INTb** and **INT** into their respective [2+2] cycloadducts **2b** (9.06 kcal·mol^{-1}) and **4** (11.06 kcal·mol^{-1}). The most effective charge delocalization is found in intermediate **INTa** (see above) and, consequently, their interacting terminal carbon atoms C2 and C8 are less polar than those of **INTb** and **INT** (see Σq in Figures 2 and 3), thus making the 4π-electrocyclic ring closure of these later intermediates easier than that of **INTa**. The partial recovery of aromaticity on going from **INTb** to **2b** can also account for the lower energy barrier of this conversion in comparison with that of **INTa** into **2a**.

It is worth emphasizing that the first energy barrier of the transformation **1a** → **2a** is lower than the second one, similar to what has been calculated for the two-step Staudinger reaction between ketenes and imines[14] and in sharp contrast with the rest of the [2+2] cycloadditions between imines and ketenimines that we have previously studied by computational methods. The particular thermodynamic stability of the cross-conjugated mesomeric betaine **INTa** may well account for this fact.

Pseudopericyclic 6π-Electrocyclic Ring Closure. The alternative reaction pathway that has been computationally analyzed for the cyclization of *N*-acylimino-ketenimines **1a**,**b** is the 6π-electrocyclic ring closure, via the transition structures **TS3a**,**b**, leading to the 1,3-oxazines **5a**,**b** (Scheme 5).

We have established the pseudopericyclic orbital topology of both transition states on the basis of their geometries, the results of the NBO analyses, and their magnetic behavior. First, the animation of the imaginary

SCHEME 5. The 6π-Electrocyclic Ring Closure of the *N*-Acylimino-ketenimines 1a,b Leading 5a,b

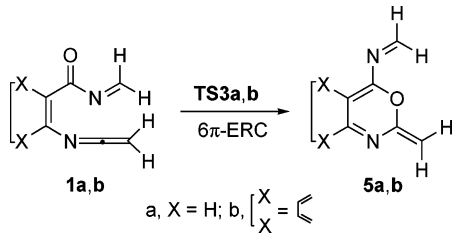

vibration of **TS3a**,**b** reveals that the nuclear motion has no component associated with the rotation around the C=O group (see the dihedral angles shown in Figures 2 and 3). Instead, the forming six-membered ring in the transition state is nearly planar, and the electronic motions correspond to the attack of a lone pair of the oxygen atom on the LUMO plane of the ketenimine component, both placed in the molecular plane, and to the slight rotation of the cumulenic C=C bond. Second, the NBO analyses of **TS3a**,**b** show bonding between an oxygen lone pair and the π^* C1−N3 natural localized orbital (the second-order perturbation energy associated with this donation being $\Delta E(2)_{\mathrm{LpO}\rightarrow\pi^*\mathrm{C1-N3}} > 42$ kcal mol^{-1}). Therefore, the new, partially formed σ-bond is due to the interaction between an sp^2-lone pair of the carbonyl oxygen atom and a p-orbital of the C=N bond placed in the molecular plane, instead of involving the two parallel p-orbitals in both termini of the cyclic array of six atoms (see Figure 4). Besides, the p-orbital at the nitrogen atom is becoming the new lone pair in the final product while the original lone pair will be the new p-orbital. Consequently, nonbonded pairs are converted into bonded pairs thus giving rise to "disconnections" in the cyclic array of overlapping orbitals, because the atomic orbitals switching functions are mutually orthogonals. These characteristics are consistent with a pseudopericyclic process. The pseudopericyclic reactions represent a special kind

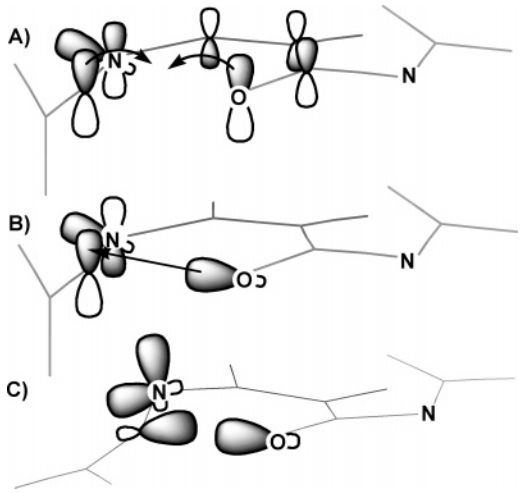

FIGURE 4. Basic atomic orbital interactions for the 6π-electrocyclic ring closure of *N*-acylimino-ketenimines **1**: (A) pericyclic pathway; (B) pseudopericyclic pathway; and (C) calculated transition state.

(13) A related tilting of a C=O group in the direction of a ketene valence isomer in mesoionic pyridopyrimidinylium olates and nonmesoionic pyridopyrimidinones has been described in: Plüg, C.; Wallfisch, B.; Andersen, H. G.; Bernharddt. P. V.; Baker, L.-J.; Clark, G. R.; Wong, M. W.; Wentrup, C. *J. Chem. Soc*., *Perkin Trans. 2* **2000**, 2096−2108.

(14) (a) Hegedus, L. S.; Montgomery, J.; Narukawa, Y.; Snustad, D. C. *J. Am. Chem. Soc*. **1991**, *113*, 5784−5791. (b) Cossío, F. P.; Ugalde, J. M.; López, X.; Lecea, B.; Palomo, C. *J. Am. Chem. Soc*. **1993**, *115*, 995−1004. (c) Lecea, B.; Arrastia, I.; Arrieta, A.; Roa, G.; López, X.; Arriortua, M. I.; Ugalde, J. M.; Cossío, F. P. *J. Org. Chem*. **1996**, *61*, 3070−3079.

of pericyclic reaction that has been placed on a solid foundation by the works of Birney and others.[10,15]

The computed energy barrier for the transformation of imino-ketenimine **1a** into **5a** was very low, 4.88 kcal·mol^{-1}, as expected for a pseudopericyclic reaction, and the process is predicted to be exothermic by 14.36 kcal·mol^{-1} (Table 1). Probably as a result of the loss of the aromaticity in the benzene ring taking place in the conversion **1b** → **5b** (note the *o*-quinoid type structure of **5b**), the calculated energy barrier of this transformation is somewhat higher than that of the preceding case (9.94 kcal·mol^{-1}). The DFT approach predicts that this process, **1b** → **5b**, is nearly isoenergetic ($\Delta E_{rxn} = -0.1$ kcal·mol^{-1}), while at the MP2/6-31G*//HF/6-31G* level it is predicted to be endoergonic ($\Delta E_{rxn} = 7.11$ kcal·mol^{-1}).

To confirm the pseudopericyclic nature of the 6π-electrocyclic ring closures of **1a**,**b** via **TS3a**,**b** affording **5a**,**b**, as well as to prove the partial loss of aromaticity of the benzene ring in the conversions **1b** → **INTb** and **1b** → **5b**, we have computed the nucleus-independent chemical shifts (NICS) at the B3LYP/6-31G* theoretical level at different points of structures **TS3a**,**b**, **1b**, **INTb**, **2b**, and **5b**. According to Schleyer,[16] large negative NICS values at the center of the ring under consideration are associated with aromatic character, whereas positive NICS values are a convenient indicator of antiaromaticity. In addition, Cossío et al.[17] demonstrated that the aromatic behavior of compounds and transition states can be described by the variation of the NICS at different points above and below the molecular plane, the intersection point being the (3,+1) ring critical point of the electron density (RCP) defined by Bader.[18] Two ring currents circulating at a certain distance from the molecular plane characterize π-aromaticity, benzene being the archetypal example.[17]

In relation to the magnetic properties of the transition structures **TS3a**,**b**, the results support its pseudopericyclic nature, given that at the RCP of **TS3a** and **TS3b** the computed NICS were 0.16 and 1.67 ppm·mol^{-1}, respectively, and both plots of the calculated NICS against *z* show a similar shape (see Figure 5A) to those described for the 6π-electrocyclic ring closure of 5-oxo-2,4-pentadienal and *N*-formyliminovinyl ketene to pyran-2-one and 1,3-oxazin-6-one, respectively, two processes unequivocally pseudopericyclic.[10a,b,19] By contrast, an aromatic disrotatory ring closure shows one ring current circulating on the side where the disrotatory movement allows a close proximity between the terminal p atomic orbitals, this kind of aromaticity being defined by Cossío as π^1-aromaticity.[17c]

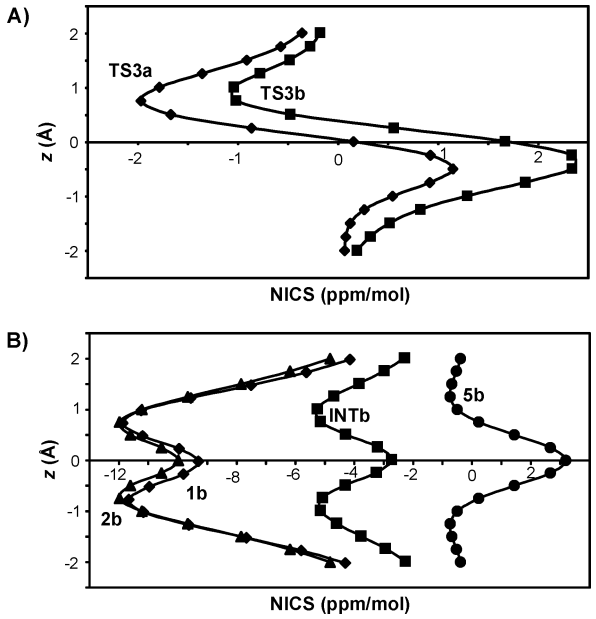

FIGURE 5. Plot of the calculated NICS versus *z* for (A) the forming six-membered ring of the transition structures **TS3a** and **TS3b** corresponding to the 6π-electrocyclic ring closure of **1a**,**b** and (B) the benzene ring of **1b**, **2b**, **INTb**, and **5b**.

On the other hand, our results show that the benzene ring of **1b** exhibits negative NICS at all the points calculated, the maximum (−11.9 ppm/mol) found at 0.73 Å above and below the ring critical point. This same pattern is shown by the benzene ring of the [2+2] cycloadduct **2b** ($NICS_{max} = -12.0$ ppm/mol at ±0.75 Å), and consequently, the benzene ring in both structures is aromatic. By contrast, the $NICS_{max}$ computed in the benzene ring of benzoxazine **5b** was 3.19 ppm/mol, therefore proving to be nonaromatic. Interestingly, the zwitterionic intermediate **INTb** showed low negative NICS, the largest value being −5.25 ppm/mol, found at 1.01 Å above and below the ring critical point, indicating that its benzene ring is only slightly aromatic (see Figure 5B).

Kinetic Analysis and Mode Selectivity in the Cyclization of Imino-ketenimines 1a,b. After having discussed the two modes of intramolecular cyclization of imino-ketenimines **1a**,**b**, [2+2] cycloaddition, and 6π-electrocyclic ring closure, let us now analyze the heights of the different energy barriers gathered in Table 1 to predict which would be the preferred reaction path. From the reaction profile in Figure 1, it seems that the [2+2] cycloadducts **2a**,**b** are predicted to be the products of thermodynamic control, while the oxazines **5a**,**b** should be the kinetically controlled products. In the transformation **1b** → **2b** and **5b**, the energy barriers ΔE_{1b}, ΔE_{2b}, and ΔE_{3b} are quite similar, and the energy barrier for the electrocyclic ring opening of the oxazine **5b** affording the imino-ketenimine **1b**, ΔE_{-3b}, is very low (10.04 kcal·mol^{-1}). For these reasons, it seems reasonable to assert that even if **5b** is the product of the kinetic control, it would be easily (and rapidly) transformed into the [2+2] cycloadduct **2b**. However, this assumption is not obvious in the transformation of **1a** into **2a** and/or **5a**, as the energy barriers ΔE_{2a} and ΔE_{3a} are quite different, and because ΔE_{-3a} is high (19.24 kcal·mol^{-1}). Therefore, we decided to carry out a quantitative kinetic analysis to predict,

(15) (a) Birney, D. M.; Xu, X.; Ham, S. *Angew. Chem., Int. Ed.* **1999**, *38*, 189−193. (b) Birney, D. M.; Ham, S.; Unruh, G. R. *J. Am. Chem. Soc.* **1997**, *119*, 4509−4517. (c) Fabian, W. M. F.; Kappe, C. O.; Bakulev, V. A. *J. Org. Chem.* **2000**, *65*, 47−53. (d) Liu, R. C.-Y.; Lusztyk, J.; McAllister, M. A.; Tidwell, T. T.; Wagner, B. D. *J. Am. Chem. Soc.* **1998**, *120*, 6247−3251. (e) Luo, L.; Bartberger, M. D.; Dolbier, W. R. *J. Am. Chem. Soc.* **1997**, *119*, 12366−12367.

(16) Schleyer, P. v. R.; Maerker, C.; Dransfeld, A.; Jiao, H.; Hommes, N. J. R. v. E. *J. Am. Chem. Soc.* **1996**, *118*, 6317−6318.

(17) (a) Morao, I.; Cossío, F. P. *J. Org. Chem.* **1999**, *64*, 1868−1874. (b) Cossío, F. P.; Morao, I.; Jiao, H.; Scheleyer, P. v. R. *J. Am. Chem. Soc.* **1999**, *121*, 6737−6746. (c) R. de Lera, A.; Alvarez, R.; Lecea, B.; Torrado, A.; Cossío, F. P. *Angew. Chem., Int. Ed.* **2001**, *40*, 557−561.

(18) Bader, R. F. W. *Atoms in Molecules−A Quantum Theory*; Clarendon Press: Oxford, UK, 1990; pp 13−52.

(19) Rodríguez-Otero, J.; Cabaleiro-Lago, E. M. *Chem. Eur. J.* **2003**, *9*, 1837−1843.

more precisely, the ratio of final products, **2a**,**b** versus **5a**,**b**, considering the mechanistic scheme represented below. It was necessary to solve the system of differential equations outlined in eqs 1−4, with the environment conditions represented in eqs 5 and 6. For simplicity, the steady-state approximation was applied to [**INT**].[20] The solutions were eqs 7−9, where λ_1 and λ_2 are a combination of the rate constants k_1, k_2, k_3, k_{-1}, and k_{-3}, which were calculated by means of the eqs 10−12 (see the Supporting Information).

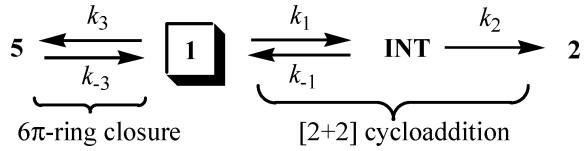

$$\frac{d[\mathbf{1}]}{dt} = -(k_1 + k_3)[\mathbf{1}] + k_{-1}[\mathbf{INT}] + k_{-3}[\mathbf{5}] \quad (1)$$

$$\frac{d[\mathbf{INT}]}{dt} = k_1[\mathbf{1}] - (k_{-1} + k_2)[\mathbf{INT}] = 0;$$

$$[\mathbf{INT}] = \frac{k_1[\mathbf{1}]}{(k_{-1} + k_2)} \quad (2)$$

$$\frac{d[\mathbf{2}]}{dt} = k_2[\mathbf{INT}] \quad (3)$$

$$\frac{d[\mathbf{5}]}{dt} = k_3[\mathbf{1}] - k_{-3}[\mathbf{5}] \quad (4)$$

$$[\mathbf{1}]_0 = [\mathbf{1}] + [\mathbf{INT}] + [\mathbf{2}] + [\mathbf{5}] \quad (5)$$

$$[\mathbf{2}]_0 = [\mathbf{INT}]_0 = [\mathbf{5}]_0 = 0 \quad (6)$$

$$[\mathbf{5}] = \frac{k_3[\mathbf{1}]_0}{(\lambda_2 - \lambda_1)}(e^{\lambda_1 t} - e^{\lambda_2 t}) \quad (7)$$

$$[\mathbf{1}] = \frac{[\mathbf{1}]_0}{(\lambda_2 - \lambda_1)}[(\lambda_2 + k_{-3})e^{\lambda_1 t} - (\lambda_1 + k_{-3})e^{\lambda_2 t}] \quad (8)$$

$$[\mathbf{2}] = \frac{k_1 k_2[\mathbf{1}]_0}{(k_2 + k_{-1})(\lambda_2 - \lambda_1)}\left[\frac{(\lambda_2 + k_{-3})(e^{\lambda_2 t} - 1)}{\lambda_2} - \frac{(\lambda_1 + k_{-3})(e^{\lambda_1 t} - 1)}{\lambda_1}\right] \quad (9)$$

$$\Delta E_{-1} = \Delta E_1 - \Delta E_{\mathbf{INT}} \quad (10)$$

$$\Delta E_{-3} = \Delta E_3 - \Delta E_{\mathrm{rxn5}} \quad (11)$$

$$k = \frac{K_B T}{h}[e^{-(\Delta E/RT)}] \quad (12)$$

In contrast with other quantitative kinetic analyses that we have previously performed,[5c,7a] the present one shows a strong dependence of the ratio **2a**,**b/5a**,**b** with the reaction time. This is a consequence of the reversibility at room temperature of the 6π-electrocyclic ring closure of **1a**,**b** leading to **5a**,**b** allowing the conversion of **5a**,**b** into **2a**,**b** under the reaction conditions.

The calculated values for the ratio [**2**]/[**5**] at various reaction times show remarkable differences between the systems **1a** → **2a/5a** and **1b** → **2b/5b**. According to our results, at 298 K, after a reaction time of 10^{-4} s the ratio **2b/5b** would be 4.6, i.e. 82.14% of **2b** vs 17.86% of **5b**; at 10^{-3} s 100% of **2b** is predicted to be in the reaction mixture. By contrast, after 3×10^3 s the ratio **2a/5a** would reach a value of 5.5, i.e. 84.5% of **2a** vs 15.5% of **5a**, and after 10^4 s the proportion of **2a** would rise to 99.8% (see Table 2 and Figure 6).

TABLE 2. Variation of the Ratio of Products 2a,b/5a,b with the Reaction Time (*t*)

t (s)	2a/5a	% 2a	*t* (s)	2b/5b	% 2b
1×10^{-4}	1.271×10^{-2}	1.27	1×10^{-20}	4.877×10^{-2}	4.65
1×10^{-2}	1.272×10^{-2}	1.27	1×10^{-10}	8.648×10^{-2}	7.96
1×10^{0}	1.334×10^{-2}	1.32	1×10^{-7}	8.767×10^{-2}	8.06
1×10^{2}	7.688×10^{-2}	7.14	1×10^{-5}	2.932×10^{-1}	22.67
3×10^{2}	2.178×10^{-1}	17.88	3×10^{-5}	8.832×10^{-1}	46.90
1×10^{3}	8.745×10^{-1}	46.65	7×10^{-5}	2.610	72.30
2×10^{3}	2.477	71.24	1×10^{-4}	4.599	82.14
3×10^{3}	5.457	84.51	2×10^{-4}	2.032×10^{1}	95.31
1×10^{4}	4.947×10^{2}	99.80	1×10^{-3}	4.492×10^{5}	100
1×10^{5}	8.752×10^{26}	100	1×10^{-2}	1.293×10^{54}	100
1×10^{6}	2.576×10^{269}	100	1×10^{-1}	∞	100

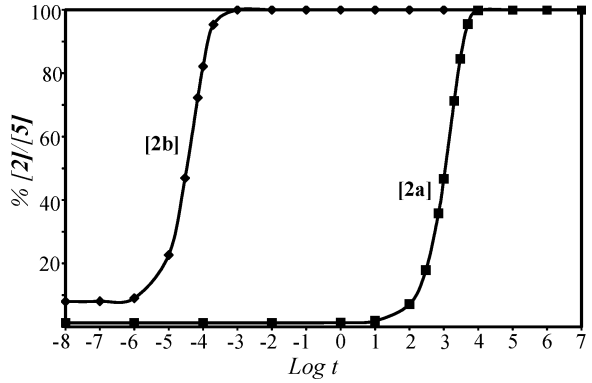

FIGURE 6. Plot of percent [**2a**] and [**2b**] (the [2+2] cycloadducts) in relation to [**5a**] and [**5b**], respectively (the products of the 6π-electrocyclic ring closure) against log *t* (time in seconds).

Accordingly, this kinetic analysis shows that the oxazines **5** are the kinetically controlled products, but they should transform rapidly and totally into the [2+2] cycloadducts **2** at room temperature. The reaction time required for the total transformation of oxazine **5a** into the [2+2] cycloadduct **2a** is approximately 3 h. By contrast, due to the different kinetic behavior of the system **1b** → **2b/5b**, both the formation of the [2+2] cycloadduct **2b** and the transformation of the initially formed oxazine **5b** into **2b** are predicted to be completed after extremely short reaction times.

In summary, this computational study predicts that the *N*-acylimino-ketenimines **1** should undergo easily an intramolecular cyclization leading to the corresponding [2+2] cycloadducts **2** via a two-step pathway. The presence of the C=O group attached to the iminic nitrogen allows for the increase of the electrophilic character of the ketenimine moiety, thus facilitating the first reaction step in relation to other imino-ketenimines supporting an sp^3-carbon atom on the iminic nitrogen. The alternative cyclization of the *N*-acylimino-ketenimines **1** consisting of a pseudopericyclic 6π-electrocyclic ring closure leading to 1,3-oxazines **5** has been mechanistically char-

(20) Espenson, J. H. *Chemical Kinetics and Reaction Mechanisms*; McGraw-Hill: New York, 1981; pp 72−87.

SCHEME 6. Synthesis of Azeto[2,1-*b*]quinazolin-8-ones 12[a]

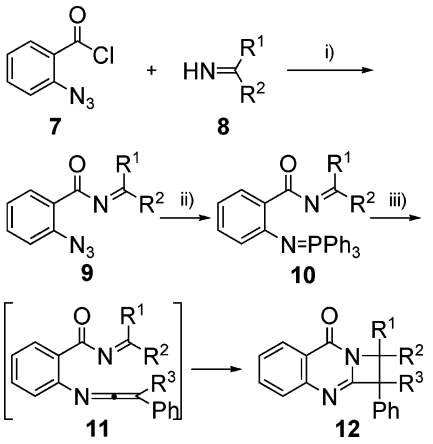

[a] Reagents and conditions: (i) Et_3N, toluene, 0 °C → rt, 2 h; (ii) PMe_3, toluene, rt, 30 min; (iii) $PhR^3C{=}C{=}O$, toluene, rt, 30 min.

acterized. The quantitative kinetic analysis shows that despite the oxazines **5** being predicted to be the kinetically controlled products, they will transform into the [2+2] cycloadducts **2** at room temperature in short reaction times.

Experimental Study

We next explored the preparation of a series of *N*-acylimino-ketenimines to check experimentally the results of the computational study.

It has been described that *N*-acylimines may be easily prepared by reaction of acyl halides either with ketimines nonsubstituted at the nitrogen atom[8b,21] or with *N*-trimethylsilylaldimines,[22] and we usually prepare ketenimines by sequential treatment of organic azides with tertiary phosphines and ketenes.[5,7] Thus, we combined these synthetic methodologies for the preparation of the requisite heterocumulenes **11** (Scheme 6). Whereas the reaction of 2-azidobenzoyl chloride **7** with *N*-trimethylsilylaldimine only gave complex mixtures, it cleanly reacted with *C*,*C*-diaryl ketimines, *C*-methyl-*C*-phenyl ketimine, and ethyl benzimidate in toluene solution at 0 °C in the presence of triethylamine, yielding *N*-acylimines **9** (Scheme 6). Treatment of a toluene solution of compounds **9** with 1 equiv of 1 M trimethylphosphane in toluene was followed by evolution of dinitrogen, indicating the conversion of the azide function into the corresponding λ^5-phosphazene **10**. The isolation and purification of compounds **10** were prevented by the extreme hydrolytic sensitivity of the phosphazene group. When these compounds were treated in the same reaction flask, at room temperature, with diphenyl ketene or methyl phenyl ketene the pale yellow reaction mixture turned orange, and immediately faded to a colorless solution. IR spectra of the reaction mixtures did not show the strong absorption around 2000 cm^{-1} expected for the C=C=N grouping of ketenimines **11**, which should reasonably result from the aza-Wittig reaction of the phosphazene with the ketene.[5b] Azeto[2,1-*b*]quinazolin-8-ones **12** were isolated from the final reaction mixtures in moderate to good yields after purification by column chromatography (Table 3). No other reaction products could be separated in appreciable yield in the chromatographic purification. Compounds **12** were unequivocally characterized by their analytical and spectral data (see the Experimental Section).

TABLE 3. 1,2-Dihydroazeto[2,1-*b*]quinazolin-8-ones 12

	R^1	R^2	R^3	yield (%)
12a	C_6H_5	C_6H_5	C_6H_5	65
12b	C_6H_5	C_6H_5	CH_3	44
12c	4-CH_3-C_6H_4	4-CH_3-C_6H_4	C_6H_5	67
12d	4-CH_3-C_6H_4	4-CH_3-C_6H_4	CH_3	44
12e	C_6H_5	CH_3	C_6H_5	58
12f	C_6H_5	OCH_2CH_3	C_6H_5	36

Obviously the formation of azetoquinazolinones **12** is rationalized as occurring by a formal intramolecular [2+2] cycloaddition between the imine and the ketenimine functions of the putative imino-ketenimines **11**, thus confirming the predictions of the computational and kinetic analyses.

Conclusions

Ab initio and DFT calculations predict that *N*-acylimino-ketenimines **1**, where the carbonyl carbon atom and the keteniminic nitrogen atom are linked either by a vinylic or an *o*-phenylene tether, should undergo easily an intramolecular cyclization leading to the corresponding [2+2] cycloadducts **2** via a two-step pathway, with formation of cross-conjugated mesomeric betaines as intermediates. The C=O group attached to the iminic nitrogen increases the electrophilic character of the ketenimine moiety, thus facilitating the first reaction step.

The alternative cyclization of the *N*-acylimino-ketenimines **1** via a 6π-electrocyclic ring closure leading to 1,3-oxazines **5** is the kinetically favored process. The pseudopericyclic character of the corresponding transition states has been established on the basis of their geometric parameters, the NBO analyses, and their nonaromatic character, as determined by the NICS values.

The quantitative kinetic analysis shows a strong dependence of the ratio [**2**]/[**5**] with the reaction time. In spite of the fact that oxazines **5** are the kinetically controlled products, they should transform into the [2+2] cycloadducts **2** at room temperature in short reaction times.

N-Acylimino-ketenimines **11**, with both reactive functions placed onto an *o*-phenylene scaffold, have been synthesized. They rapidly converted into azeto[2,1-*b*]-quinazolin-8-ones **12** in moderate to good yields, by a formal [2+2] cycloaddition between the imine and ketenimine functions.

Experimental Section

Materials. 2-Azidobenzoyl cloride **7**,[23] diphenyl ketimine,[24] bis(4-methylphenyl) ketimine,[23] phenylmethyl ketimine,[23] eth-

(21) Kupfer, R.; Nagel, M.; Würthwein, E.-U.; Allmann, R. *Chem. Ber.* **1985**, *118*, 3089−3104.
(22) Kupfer, R.; Meier, S.; Würthwein, E.-U. *Synthesis* **1984**, 688−699.
(23) Porter, T. C.; Samalley, R. K.; Teguiche, M.; Purwono, B. *Synthesis* **1997**, 773−777.
(24) Pickard, P. L.; Tolbert, T. L. *J. Org. Chem.* **1961**, *26*, 4886−4888.

yl iminobenzoate hydrochloride,[25] diphenylketene,[26] and methylphenylketene[27] were prepared by published procedures.

Preparation of 1,2-Dihydroazeto[2,1-*b*]quinazolin-8-ones 12 (General Procedure). The corresponding imine or imidate (4 mmol) was dissolved in dry toluene (25 mL) and cooled at 0 °C before the dropwise addition of a solution of 2-azidobenzoyl chloride **7** (0.73 g, 4 mmol) in the same solvent (5 mL). The reaction mixture was stirred at 0 °C for 30 min. At this point, triethylamine (0.6 g, 6 mmol) was added, and the stirring was continued for 2 h at room temperature. The precipitated triethylammonium chloride was separated by filtration, and the solvent was removed from the filtrate under reduced pressure. The resulting oil was purified by column chromatography on silica gel, using hexanes/ethyl acetate (7:3, v/v) as eluent, except for **9e** ($R^1 = C_6H_5$; $R^2 = CH_3$) where the crude material was used us such in the following step.

To a solution of the corresponding *N*-acylimine **9** (3 mmol) in dry toluene (15 mL) was added trimethylphosphane (1 M toluene solution, 3 mL, 3 mmol), and the reaction mixture was stirred at room temperature for 30 min. Then a solution of the appropriate ketene (3 mmol) in dry toluene (2 mL) was added, and the stirring was continued for 30 min. The solvent was removed under reduced pressure and the crude material was purified by column chromatography on silica gel, using hexanes/ethyl acetate (4:1, v/v) as eluent.

Computational Methods. The calculations were performed with the Gaussian98 suite of programs.[28] Geometry optimizations were carried out at the RHF, Becke3LYP,[29] and MP2[30] theoretical levels with the internal 6-31G* basis set.[31] Harmonic frequency calculations at each level of theory verified the identity of each stationary point as a minimum or a transition state, and were used to provide an estimation of the zero-point vibrational energies (ZPVE), which were not scaled. Bond orders[32] and natural charges were calculated with the NBO (natural bond orbital) method.[33] NICS values were obtained at the B3LYP/6-31G*// B3LYP/6-31G* level with the GIAO (Gauge-Independent Atomic Orbital) method.[34]

Acknowledgment. This work has been supported by the MCYT-FEDER (Project BQU2001-0010) and the Fundación Seneca-CARM (Proyecto PI-100749/FS/01). P.S.-A. thanks the Universidad de Murcia for a studentship. The valuable comments of Prof. F. P. Cossío are also acknowledged.

Supporting Information Available: Tables S1−S7 including the chief geometric, electronic, and energetic features for all stationary points discussed in the text; Cartesian coordinates of local minima and transition structures discussed in the text, selected orbital interactions of the NBO analysis, mathematical treatment of the kinetic analysis and analytical and spectroscopic data for compounds **12a**−**f**. This material is available free of charge via the Internet at http://pubs.acs.org.

JO0482716

(25) MacKenzie, C. A.; Schmidt, G. A.; Webb, L. R. *J. Am. Chem. Soc.* **1951**, *73*, 4990.

(26) Taylor, E. C.; Mckillop, A.; Hawks, G. H. *Org. Synth.* **1973**, *52*, 36−38.

(27) Pracejus, H.; Wallura, G. *J. Prakt. Chem.* **1962**, *19*, 33−36.

(28) Frisch, M. J.; Trucks, G. W.; Schlegel, H. B.; Scuseria, G. E.; Robb, M. A.; Cheeseman, J. R.; Zakrzewski, V. G.; Montgomery, J. A., Jr.; Stratmann, R. E.; Burant, J. C.; Dapprich, S.; Millam, J. M.; Daniels, A. D.; Kudin, K. N.; Strain, M. C.; Farkas, O.; Tomasi, J.; Barone, V.; Cossi, M.; Cammi, R.; Mennucci, B.; Pomelli, C.; Adamo, C.; Clifford, S.; Ochterski, J.; Petersson, G. A.; Ayala, P. Y.; Cui, Q.; Morokuma, K.; Malick, D. K.; Rabuck, A. D.; Raghavachari, K.; Foresman, J. B.; Cioslowski, J.; Ortiz, J. V.; Stefanov, B. B.; Liu, G.; Liashenko, A.; Piskorz, P.; Komaromi, I.; Gomperts, R.; Martin, R. L.; Fox, D. J.; Keith, T.; Al-Laham, M. A.; Peng, C. Y.; Nanayakkara, A.; Gonzalez, C.; Challacombe, M.; Gill, P. M. W.; Johnson, B.; Chen, W.; Wong, M. W.; Andres, J. L.; Gonzalez, C.; Head-Gordon, M.; Repogle, E. S.; Pople, J. A. *Gaussian 98*, revision A.5; Gaussian, Inc.: Pittsburgh, PA, 1998.

(29) (a) Parr, R. G.; Yang, W. *Density-Functional Theory of Atoms and Molecules*; Oxford University Press: New York, 1989. (b) Bartolotti, L. J.; Fluchichk, K. *Reviews in Computational Chemistry* Lipkowitz, K. B., Boyds D. B., Eds. VCH Publishers: New York, 1996; , Vol. 7, pp 187−216. (c) Kohn, W.; Becke, A. D.; Parr, R. G. *J. Phys. Chem.* **1996**, *100*, 12974−12980. (d) Ziegler, T. *Chem. Rev.* **1991**, *91*, 651−667.

(30) (a) Moller, C.; Pleset, M. S. *Phys. Rev.* **1934**, *46*, 618−622. (b) Frisch, M. J.; Head-Gordon, M.; Pople, J. A. *Chem. Phys. Lett.* **1990**, *166*, 281−289. (c) Frisch, M. J.; Head-Gordon, M.; Pople, J. A. *Chem. Phys. Lett.* **1990**, *166*, 275−280. (d) Binkley, J. S.; Pople, J. A. *Int. J. Quantum Chem.* **1975**, *9*, 229−236. (e) Pople, J. A.; Binkley, J. S.; Seeger, R. *Int. J. Quantum Chem. Symp.* **1976**, *10*, 1−19.

(31) Hehre, W. J.; Radom, L.; Schleyer, P. v. R.; Pople, J. A. *Ab Initio Molecular Orbital Theory*; Wiley: New York, 1986; pp 71−82 and references therein.

(32) Wiberg, K. B. *Tetrahedron* **1968**, *24*, 1083−1096.

(33) (a) Redd, A. E.; Weinstock, R. B.; Weinhold, F. *J. Chem. Phys.* **1985**, *83*, 735−746. (b) Reed, A. E.; Curtiss, L. A.; Weinhold, F. *Chem. Rev.* **1988**, *88*, 899−926. (c) Reed, A. E.; Scheleyer, P. v. R. *J. Am. Chem. Soc.* **1990**, *112*, 1434−1445.

(34) Wolinski, K.; Hilton, J. F.; Pulay, P. *J. Am. Chem. Soc.* **1990**, *112*, 8251−8260.